Physical Communication 30 (2018) 15–25

Contents lists available at ScienceDirect

Physical Communication

journal homepage: www.elsevier.com/locate/phycom

Full length article

Adaptive dual-mode OFDM with index modulation

Sultan Aldırmaz Çolak [a,*], Yusuf Acar [b,c], Ertugrul Basar [d]

[a] Kocaeli University, Department of Electronics and Communication Engineering, 41380, Kocaeli, Turkey
[b] Wireless Technology Center, Purdue University-Fort Wayne, USA
[c] Department of Electrical and Electronics Engineering, Istanbul Kultur University, 34156 Bakirkoy, Istanbul, Turkey
[d] Istanbul Technical University, Faculty of Electrical and Electronics Engineering, 34469 Maslak, Istanbul, Turkey

ARTICLE INFO

Article history:
Received 9 November 2017
Received in revised form 8 June 2018
Accepted 8 July 2018

Keywords:
OFDM-IM
Dual mode OFDM-IM
Adaptive-OFDM
Spectral efficiency

ABSTRACT

With the integration of the index modulation concept, the popular OFDM has gained an appealing new dimension. However, OFDM with index modulation (OFDM-IM) causes a decrease in data rate for higher order modulations due to its unused subcarriers. Recently, dual-mode OFDM with index modulation (DM-OFDM-IM) has been proposed to prevent this decrease in data rate. The spectral efficiency (SE) of both techniques depends on the selection of different parameters, such as modulation types and number of active subcarriers. However, the quality of the wireless channel has not been taken into account yet to increase the data rate. In this paper, we propose a new adaptive DM-OFDM-IM (A-DM-OFDM-IM) system to enhance the bit error probability (BER) performance considering the channel conditions and obtain a substantial increase in SE. Unlike the previous DM-OFDM-IM and the classical OFDM-IM schemes, our proposed system enables the use of different types of modulations for different subblocks in one OFDM signal. We demonstrate that the SE of the proposed system is comparable with that of its OFDM-IM and DM-OFDM-IM counterpart under frequency selective Rayleigh channels. Moreover, computer simulations corroborate that the derived theoretical results are considerably accurate for the SE of A-DM-OFDM-IM systems.

1. Introduction

OFDM has been widely used in several different wireless systems, such as Long Term Evolution (LTE) and Mobile Worldwide Interoperability Microwave Systems (WiMAX), and has become the most popular waveform in the past decade. One of the main advantages of OFDM systems is the conversion of frequency selective channels into frequency flat channels. Since each of the available subcarriers experiences flat fading, one-tap equalizer is enough for compensating the channel effect. Another important property of OFDM is its easy implementation owing to FFT/IFFT operations. In addition to having excellent properties, OFDM has also some drawbacks, such as high peak to average power ratio (PAPR), high out-of-band emission, etc. Nonetheless, OFDM is one of the strongest candidates for being used in the next-generation wireless communication systems as well due its appealing advantages and backward compatibility. Consequently, researchers have investigated numerous modifications to OFDM systems in order to enhance its spectral efficiency (SE).

Due to the disadvantages of OFDM, several new potential waveforms have been proposed for next-generation wireless communication systems, such as filter bank multicarrier (FBMC), generalized frequency division multiplexing (GFDM) and filtered OFDM (f-OFDM) etc [1,2]. However, the performance improvement provided by these techniques is relatively limited beside the computational complexity they bring, and therefore, operators are still eager to continue using OFDM for next-generation wireless communication systems [2].

Multiple-input multiple-output (MIMO) technology has been integrated to OFDM in LTE systems, thereby the SE increases with the number of antennas used in transmitter (Tx) and receiver (Rx) sides. As an emerging MIMO solution, spatial modulation (SM) has been proposed in [3] and a part of data bits is transmitted by selecting the indices of the active transmit antennas. In SM system, SE is increased by the base-two logarithm of the total number of transmit antennas compared to classical systems employing signal constellations such as M-ary phase shift keying (M-PSK) or M-ary quadrature amplitude modulation (M-QAM). Recently, Basar et al. introduced a novel OFDM system, namely OFDM with index modulation (OFDM-IM), which is one of the promising techniques to increase SE without any degradation in bit error rate (BER) performance [4]. This scheme uses not only OFDM subcarriers, but also the positions of these subcarriers for data transmission. As a

* Corresponding author.
E-mail addresses: sultan.aldirmaz@kocaeli.edu.tr (S.A. Çolak), acary@ipfw.edu, y.acar@iku.edu.tr (Y. Acar), basarer@itu.edu.tr (E. Basar).

https://doi.org/10.1016/j.phycom.2018.07.010
1874-4907/

result, this technique can be thought of as a combination of SM and OFDM systems. According to this technique, the overall OFDM block is divided into certain number of subblocks. There are n available subcarriers in each subblock; however only k out of these n subcarriers are active, and the others are left empty (not used). Active subcarriers of each group are chosen by different mapping techniques, and then, the remaining bits are modulated with the modulation scheme and resulting data symbols are assigned to the active subcarriers.

In a short period of time, the OFDM-IM structure has not only attracted significant attention but also it has been applied to many areas where OFDM is widely used, such as visible light communications (VLC) [5,6], and MIMO systems [7–10]. Specifically, OFDM with generalized index modulation is proposed in [11] by applying a more flexible subcarrier activation procedure. Block interleaving is considered for OFDM-IM in [12] to improve its error performance. To further improve the diversity order of plain OFDM-IM, coordinate interleaving is introduced in [13]. Similarly, the authors of [14] proposed a linear constellation precoded OFDM-IM scheme to obtain additional diversity gains. Furthermore, OFDM-IM has also triggered to introduction of new IM-aided waveforms such as generalized frequency division multiplexing with IM [15]. Interested readers are referred to [16] and the references therein for a review of OFDM-IM systems.

Due to its empty subcarriers, SE of OFDM-IM can be relatively limited for higher order modulations. Recently, dual-mode OFDM-IM (DM-OFDM-IM) has been proposed to deal with this problem in [17]. In contrast to OFDM-IM, all carriers within the entire subblock are used to transfer data in DM-OFDM-IM. Moreover, unlike OFDM-IM, two different distinguishable constellations (*Cons A* and *Cons B*) are used. In DM-OFDM-IM, the overall bit block is divided into data bits and index bits as in OFDM-IM. The basic idea of DM-OFDM-IM is the utilization of all subcarriers of an OFDM symbol in order to transmit modulated symbols with two different constellations. Furthermore, the positions of the data symbols of each subblock employing different constellations are also used for data transmission. In other words, the index bits specify the positions in the OFDM subblock for symbols that are modulated with *Cons A*, and the symbols modulated with *Cons B* are placed in the remaining positions from *Cons A*. The Rx of both structures, can use maximum likelihood (ML) detector in order to estimate the transmitted bits.

A generalized DM-OFDM-IM scheme is introduced recently in [18] to increase the SE of the classical DM-OFDM-IM at the cost of negligible performance loss compared to that of DM-OFDM-IM system. Since the number of *Cons A* symbols and *Cons B* symbols are same in the classical DM-OFDM-IM scheme, the length of IM bits is also equal for each constellation alphabet. By using a variable size of the selected indices vector (I_A), possible realizations of OFDM subblocks are increased, thus the number of total transmitted bits and also the computational complexity of the ML detector increase. According to the computer simulation results of [18], for a BER value of 10^{-3}, the SE is increased by 20% compared to classical DM-OFDM-IM, at the cost of 2 dB BER degradation under a frequency selective Rayleigh channel. Even more recently, a multiple-mode OFDM-IM scheme is proposed in [19] by employing multiple distinguishable constellations in each subblock and using the full permutations of modes to carry IM bits.

In conventional OFDM, the same modulation scheme is employed on all subchannels. Nevertheless, the effects of channel are different for each subchannel, thus, the resulting BER is also different. To increase the overall BER performance of the system, adaptive modulation has been proposed as an emerging solution.

Adaptive bit loading (or adaptive modulation scheme), is a technique in which the number of bits (modulation order) carried on each subcarrier changes according to the SNR of the individual subcarrier. There are three different bit loading algorithms that use three different parameters such as BER, SE and transmit power [20]. The difference among these algorithms is that each of them tries to optimize one of these parameters under the constraints of the other two.

In the literature, there are many studies on adaptive OFDM systems [21–30]. Czylwik proposed a solution to mitigate the frequency selective fading effect on the OFDM signal in [22]. This solution is based on the fact that different modulation schemes are employed for the individual subcarriers of the OFDM signal in frequency domain according to SNR value. Thus, when the SNR value of a subcarrier is low, a low order modulation is applied to it, whereas when SNR is high, a high order modulation, *i.e.*, 256-QAM, is used. In [23], Piazzo proposed a bit loading algorithm for OFDM systems. In that study, different modulation modes and transmit powers are applied to OFDM subcarriers. Then, Zhou et al. proposed adaptive modulation for MIMO systems under perfect channel state information (CSI) and imperfect CSI conditions [24]. Singular value decomposition (SVD) is applied to the MIMO channel and it is decomposed into parallel streams. Later, the same authors proposed a nonlinear constrained optimization problem. To increase average SE (ASE), transmit power and SE at each eigen subchannel are varied according to the fading channel under average transmit power and instantaneous BER constraints. For further details on this topic, the interested readers are referred to [25–28]. Moreover, LTE systems already use adaptive modulation according to channel quality indicator (CQI) to determine the modulation order. Thus, the system can support more data rate when CQI is high.

Adaptive modulation has been proposed for the SM technology where the parameters of the Tx are dynamically adapted to the changing channel conditions [29,30]. In [30], Yang et al. proposed an optimal hybrid-SM technique, which determines the modulation level as well as the active antenna by using a limited feedback channel in order to improve the performance of classical SM systems. A similar study [29] is performed by Bouida et al. in which the SE can be maximized or average BER can be enhanced. The authors showed a trade-off between SE and average BER. When SE is to be maximized, according to a feedback channel from the Rx, the maximum modulation mode that can be used with each antenna is determined, whereas when the average BER is to be improved, the minimum modulation mode that can be achieved by all antennas is determined. Then, the Tx uses the same modulation during a given time slot.

To the best of our knowledge, there exists no efficient and computationally feasible adaptive structure (according to the channel variations) in the literature for OFDM-IM based systems in order to enhance BER and the SE.

In this paper, we propose a novel structure by merging adaptive OFDM and dual-mode OFDM with IM structures according to the channel conditions in order to enhance BER and SE for the DM-OFDM-IM system.

The main contributions of the paper are summarized as follows:

- For the first time in the literature, dual-mode OFDM-IM meets an adaptive structure with the proposed adaptive OFDM-based system.
- In this scheme, modulation type is determined according to the average SNR of each OFDM subgroup. Under constant transmitted power, we propose six threshold set values and compare the BER performance and SE values without any optimization process. The transmitter chooses modulation type according to channel variations by using the limited feedback knowledge in order to increase SE.
- It has been shown that an interesting trade-off exists between SE and the average BER. Theoretical SE values are obtained and computer simulations confirm that the derived theoretical SE values are considerably accurate for the DM-OFDM-IM systems.

Table 1
Meaning of parameters and symbols.

Parameters	Definition
m	Number of information bits for the transmission of each OFDM block
g	Number of groups each containing p bits
p	Number of bits per group (i.e., $p = m/g$)
N	Number of OFDM subcarriers
N_{CP}	Length of cyclic prefix
$\mathbf{W}_N$	Discrete Fourier transform (DFT) matrix
K	Total number of active subcarriers (*i.e.* $K = kg$)
n	OFDM subblock of length (*i.e.* $n = N/g$)
k	Number of active subcarriers in each subblock
p_1	Total number of bits that are mapped onto the active indices in each subblock
p_2	Total number of bits that are mapped onto the M-ary signal constellation in each subblock (*i.e.* $p_2 = klog_2M$)
m_1	The total number of information bits carried by the positions of the active indices in the OFDM block
m_2	The total number of information bits carried by the M-ary signal constellation symbols
I_β	Selected indices for subblock β
s_β	Modulated symbol for subblock β
$\rho_{ins,\beta}$	The average instantaneous received SNR values of subblock β
γ	Threshold for modulation selection

- The impact of imperfect feedback channel on the performance of the proposed system is considered to model real-life communication scenarios.

The rest of the paper is organized as follows: Section 2 provides a brief introduction on OFDM-IM and DM-OFDM-IM schemes. Then, the proposed scheme is presented in Section 3. Section 4 gives computer simulation results. Finally, we provide our concluding remarks in Section 5.

Notation: Throughout the paper, we use the following notation. While scalar values are italicized, vectors/matrices are presented by bold lower/upper case symbols. The transpose and the conjugate transpose are denoted by $(\cdot)^T$ and $(\cdot)^H$, respectively. $\lfloor . \rfloor$, $E\{.\}$ and $C(.,.)$ represent the floor operation, expectation notation, and Binomial coefficient. Finally, $\mathbf{W}_N$ is the discrete Fourier transform (DFT) matrix. Likewise, variables (system parameters), which are used in the paper, are summarized in Table 1.

2. Preliminaries

In this section, OFDM-IM and DM-OFDM-IM structures are reviewed to provide some background information for the proposed scheme, namely adaptive DM-OFDM-IM. Then, in the next section, A-DM-OFDM-IM is presented and its performance is compared with that of OFDM-IM and DM-OFDM-IM in terms of computational complexity and spectral efficiency.

2.1. OFDM-IM

OFDM-IM is a recently proposed technique, which uses a new basis for data transmission in addition to the employed modulation scheme. It transmits data by using active subcarrier indices and signal constellations such as M-ary PSK/QAM. This new base is responsible for the selection of active subcarriers, which carry data symbols in subblocks of an OFDM signal according to index selection bits. Thus, a number of subcarriers can be active (carrying symbols) or inactive in OFDM-IM. The SE (*i.e.*, the total number of bits to be transmitted in the OFDM signal) can be changed according to the selection of the number of active subcarriers (k), the total number of subcarriers (n) in each subblock, and also the modulation type. The system model of OFDM-IM is given in Fig. 1 [4].

In Fig. 1, m-length data sequence is divided into g groups, each containing $p = m/g$ bits. Let us assume that the OFDM symbol has N subcarriers and these subcarriers are divided into subblocks with length $n = N/g$. Out of n available subcarriers, k of them are activated according to the index selecting bits and these subcarriers are used in for data transmission through ordinary M-ary modulation. As a result, the total transmitted bits of each subblock can be calculated as

$$\lfloor \log_2(C(n,k)) \rfloor + \log_2(M)k. \tag{1}$$

Table 2
A look-up table of OFDM-IM scheme for $n = 4$, $k = 2$, $p_1 = 2$ [4].

Bits	Indices	Subblocks
[0, 0]	{1,2}	$[s_1, s_2, 0, 0]^T$
[0, 1]	{2,3}	$[0, s_1, s_2, 0]^T$
[1, 0]	{3,4}	$[0, 0, s_1, s_2]^T$
[1, 1]	{1,4}	$[s_1, 0, 0, s_2]^T$

The first and second parts of (1) stand for the number of bits that can be conveyed by active subcarrier indices and the number of bits that can be transmitted over k active subcarriers, respectively. Table 2 shows the active subcarrier indices of a subblock according to information bits. As can be seen from Table 2, if parameters are chosen as $n = 4$ and $k = 2$, the incoming bit sequence [0, 0] activates the first and the second subcarriers (where s_1 and s_2 are two modulated symbols), and these subcarriers transmit modulated symbols. The others (inactive subcarriers) are not used, thus their values are equal to 0.

Let $\mathbf{x}_F$ be the transmitted symbols of the OFDM-IM scheme by concatenating these g subblocks:

$$\mathbf{x}_F = [x(1), x(2), \ldots, x(N)]^T. \tag{2}$$

Then, inverse fast Fourier transform (IFFT) is applied to the signal as in the classical OFDM:

$$\mathbf{x}_T = \frac{N}{\sqrt{K}} \mathbf{W}_N^H \mathbf{x}_F, \tag{3}$$

where $\mathbf{x}_T$ is the time domain OFDM block, $\mathbf{W}_N$ is the discrete Fourier transform (DFT) matrix with $\mathbf{W}_N^H \mathbf{W}_N = N\mathbf{I}_N$, K is the total number of active subcarriers *i.e.*, $K = kg$), and $N/\sqrt{K}$ term is used for the normalization $E\{\mathbf{x}_T^H \mathbf{x}_T\}$=$N$.

After DFT operation, CP is added to prevent inter-symbol interference (ISI) due to channel impulse response (CIR). Then, the CP added signal is converted from parallel to serial and digital signal is transformed to an analog one, at the resulting signal is sent through the channel. The vector of CIR coefficients is given

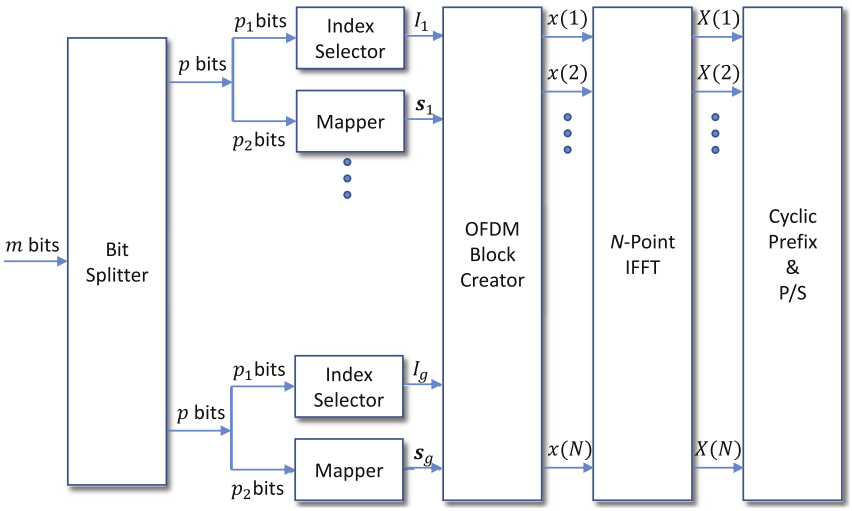

Fig. 1. System model of OFDM-IM [4].

as $\mathbf{h} = [h_1, h_2, \ldots h_v]^T$, whose elements are circularly symmetric complex Gaussian random variables with 0 mean and $1/v$ variance, *i.e.*, $\mathcal{CN}(0, 1/v)$. The channel is assumed to be constant over an OFDM symbol block. Thus, the received signal in frequency domain is expressed as

$$y_f(\alpha) = h_F(\alpha)x(\alpha) + w_F(\alpha), \tag{4}$$

where $y_F(\alpha)$, $h_F(\alpha)$, and $w_F(\alpha)$ are the received signals, the channel fading coefficients and the noise samples in the frequency domain, whose vector presentations are given as $\mathbf{y}_F$, $\mathbf{h}_F$ and $\mathbf{w}_F$, respectively. To estimate the data from the received signal, ML detector can be used in Rx for each OFDM-IM subblock. Owing to CIR knowledge, in order to estimate the active indices ($\hat{I}_\beta$) and the modulated symbols ($\hat{\mathbf{s}}_\beta$) in each subblock together, the minimum Euclidean distance between the received signal and the corrupted-transmitted signal is aimed to be obtained. Then, an estimate of the active indices and data symbols are obtained as follows:

$$\left(\hat{I}_\beta, \hat{\mathbf{s}}_\beta\right) = \arg\min_{I_\beta, s_\beta} \sum_{\gamma=1}^{k} \left|y_F^\beta(i_{\beta,\gamma}) - h_F^\beta(i_{\beta,\gamma})s_\beta(\gamma)\right|^2 \tag{5}$$

where $i_{\beta,\gamma}$, $y_f^\beta(i_{\beta,k})$ and $h_f^\beta(i_{\beta,k})$ denote the indices corresponding to active indices set of $I_\beta = \{i_{\beta,1}, \ldots, i_{\beta,k}\}$, the received signals and the corresponding fading coefficients for the subblock β, respectively. $\mathbf{s}_\beta$ represents the vector of modulated symbols from constellation alphabets.

2.2. Dual-mode OFDM-IM

The unused subcarriers reduce the SE of OFDM-IM inevitably. Recently, DM-OFDM-IM is proposed to increase the SE of OFDM-IM by utilizing the unused subcarriers [17]. However, the total transmitted power is also increased, because all subcarriers are active in DM-OFDM-IM unlike OFDM-IM. The only difference between the block diagram of OFDM-IM and DM-OFDM-IM is that the mapper block in Fig. 1 is modified as shown in Fig. 2. The incoming p_2 bits are divided into two parts each having $p_2/2$ bits. Then, each block is modulated with the selected modulation with two different constellations, namely *Cons A* and *Cons B*. Table 3 shows a look-up table for DM-OFDM-IM and shows the modulation type of a subcarrier according to the index bits [17]. For example, when index bits are [0, 0], *Cons A* is used for the first two subcarriers, and then the others are modulated by *Cons B* in the corresponding subblocks. As it can be seen from Table 3, it is very similar to Table 2, and the main difference is the utilization of a second signal constellation instead of the zeros in the subblocks.

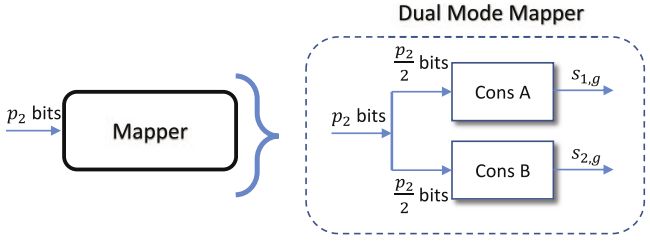

Fig. 2. Comparison of mapping principles for OFDM-IM and DM-OFDM-IM schemes.

Table 3
A look-up table of DM-OFDM-IM scheme for $n = 4$, $k = 2$, and $p_1 = 2$ [17].

Bits	Indices	Subblocks
[0, 0]	{1,2}	$[s_{1,A}, s_{2,A}, s_{1,B}, s_{2,B}]^T$
[0, 1]	{2,3}	$[s_{1,B}, s_{1,A}, s_{2,A}, s_{2,B}]^T$
[1, 0]	{3,4}	$[s_{1,B}, s_{2,B}, s_{1,A}, s_{2,A}]^T$
[1, 1]	{1,4}	$[s_{1,A}, s_{1,B}, s_{2,B}, s_{2,A}]^T$

First, as in OFDM-IM, m-length data sequence is split into g groups each group containing p bits. Then, in each group, p_1 of p bits are transferred to the index selector, and the remaining $p_2 = p - p_1$ bits are reserved to obtain the modulated symbols. Let us assume that k and $(n-k)$ subcarriers of a subblock are modulated with *Cons A* and *Cons B*, respectively. The number of IM bits is calculated as

$$p_1 = \lfloor \log_2 C(n, k) \rfloor, \tag{6}$$

where n and k represent the number of subcarriers of each group and number of symbols that are modulated with *Cons A*, respectively. The number of ordinary modulated bits is calculated as

$$p_2 = k\log_2(M_A) + (n-k)\log_2(M_B), \tag{7}$$

where M_A and M_B are the modulation orders of *Cons A* and *Cons B*, respectively. Consequently, the total number of bits of each group can be calculated as $p = p_1 + p_2$.

After index bits and symbols are obtained, OFDM signal is generated by using N-point IFFT. Then, CP is added to the OFDM signal to prevent ISI due to channel effect. To determine the difference between constellations A and B in Rx side, different power levels are used.

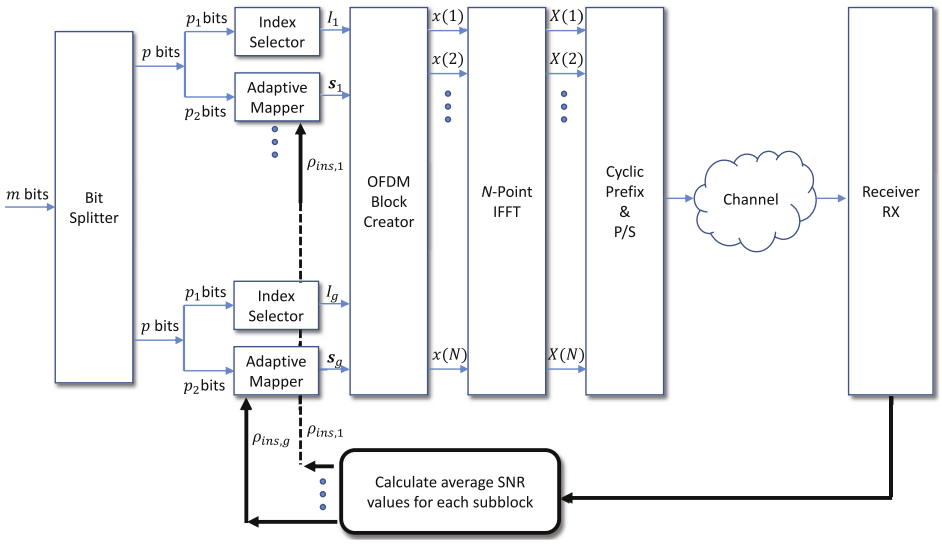

Fig. 3. The system model of the proposed A-DM-OFDM-IM system.

The SE of DM-OFDM-IM is calculated as:

$$\eta = \frac{(p_1 + p_2)g}{(N + N_{CP})}, \tag{8}$$

where N and N_{CP} are the IFFT size and length of CP, respectively.

For example, if we choose system parameters as $n = 4$, $k = 2$, $N = 128$ and $N_{CP} = 16$ and QPSK modulation is employed, *i.e.*, $M_A = M_B = 4$, the SE is obtained as 2.22 bit/s/Hz.

3. System model

3.1. The proposed scheme

The proposed A-DM-OFDM-IM system can be considered as a combination of adaptive modulation and DM-OFDM-IM. Unlike DM-OFDM-IM, the modulation order, which depends on the instantaneous received SNR, can be changed flexibly for each subblock. As a result, the proposed system enables the increase of the SE and also the BER performance when the instantaneous received SNR is high enough. As in DM-OFDM-IM, the same modulation is used in each subblock with two different constellations (*Cons A* and *Cons B*) in the proposed scheme.

Our system model is given in Fig. 3. First, we split the incoming m bits into subblocks with p length. For each subblock, we have two components, *i.e.*, the index selector and the adaptive mapper. The first p_1 bits are used to determine the positions of the modulated symbols with *Cons A*. The adaptive mapper block, which is given in Fig. 4, is responsible for the construction of the symbols from p_2 bits according to the selected modulation type with two different constellation alphabets (schemes), *i.e.*, *Cons A* and *Cons B*. The new adaptive mapper block includes modulation order selection block unlike DM-OFDM-IM.

Modulation type selection, which depends on the instantaneous received SNR of the channel, is the key point of our scheme and it is performed in the mapper block by using a limited feedback channel information. This limited feedback information includes the average instantaneous received SNR values of each subblock and the AWGN noise power. Then, indices set I_β and data symbols vector $\mathbf{s}$ are sent to OFDM block creator and N-point IFFT is applied. At last, CP is added to the OFDM signal and the resulting signal is converted from parallel to serial, and then, is transformed from digital to analog.

Fig. 5 illustrates constellations of the considered modulation schemes, and also Gray coding schemes for QPSK and 16-QAM. To

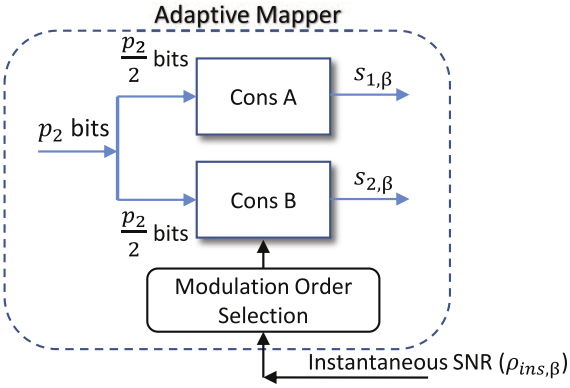

Fig. 4. The adaptive mapper block of the proposed algorithm.

determine the difference between constellations *A* and *B* in Rx side, different power levels are used. These constellation diagrams are same which are used in DM-OFDM-IM, the only difference is all constellation alphabets (*Cons A* and *Cons B*) for each modulation are normalized to have unit average energy.

We define the SNR as $\rho = E_s/N_0$ where E_s and N_0 are the average transmitted energy per symbol and the noise variance in the time domain, respectively. Also, the instantaneous received SNR of each subcarrier is defined as $\rho_{ins}(\alpha) = |h_F(\alpha)|^2 E_s/N_0$, where $h_F(\alpha)$ is the frequency-domain channel coefficient for subcarrier α.

If we use the same modulation order for all subblocks in one OFDM symbol, each subblock shows different BER performance. However, if we can choose the suitable modulation type for each subblock according to the $\rho_{ins,\beta}$ value, BER performance can be enhanced. Also, higher order modulation can be used where subblocks are exposed to low-level fading compared to high-level one, to improve the SE. Thus, modulation type is determined adaptively by comparing these values with set of threshold values. These threshold set values can be chosen with a deterministic way.

At Rx, we split the frequency response of the channel into g subblocks and calculate the average instantaneous received SNR ($\rho_{ins,\beta}$) value for n samples of each group (subblock). Then, by using the limited feedback channel, this information is sent to Tx. At Tx, the adaptive mapper block determines the modulation scheme, which is applied for each group, by comparing the average

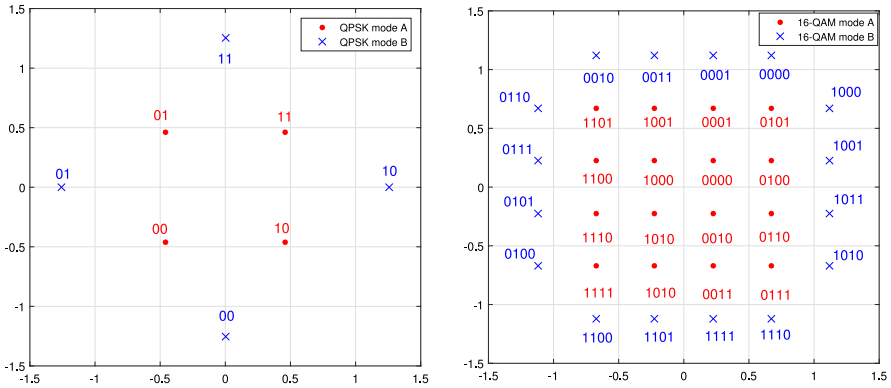

(a) QPSK constellation (b) 16-QAM constellation

Fig. 5. Normalized constellation alphabets with Gray coding of the A-DM-OFDM-IM.

Table 4
Different threshold set values considering in the paper for modulation order selection.

Cases	BPSK	QPSK	16-QAM
Case 1 $\{\gamma_1 = 18$ dB, $\gamma_2 = 10$ dB$\}$	$\rho_{ins,\beta} < 10$ dB	$10 \leq \rho_{ins,\beta} < 18$ dB	$\rho_{ins,\beta} \geq 18$ dB
Case 2 $\{\gamma_1 = 24$ dB, $\gamma_2 = 10$ dB$\}$	$\rho_{ins,\beta} < 10$ dB	$10 \leq \rho_{ins,\beta} < 24$ dB	$\rho_{ins,\beta} \geq 24$ dB
Case 3 $\{\gamma_1 = 24$ dB, $\gamma_2 = 15$ dB$\}$	$\rho_{ins,\beta} < 15$ dB	$15 \leq \rho_{ins,\beta} < 24$ dB	$\rho_{ins,\beta} \geq 24$ dB
Case 4 $\{\gamma_1 = 30$ dB, $\gamma_2 = 10$ dB$\}$	$\rho_{ins,\beta} < 10$ dB	$10 \leq \rho_{ins,\beta} < 30$ dB	$\rho_{ins,\beta} \geq 30$ dB
Case 5 $\{\gamma_1 = 30$ dB, $\gamma_2 = 15$ dB$\}$	$\rho_{ins,\beta} < 15$ dB	$15 \leq \rho_{ins,\beta} < 30$ dB	$\rho_{ins,\beta} \geq 30$ dB
Case 6 $\{\gamma_1 = 30$ dB, $\gamma_2 = 20$ dB$\}$	$\rho_{ins,\beta} < 20$ dB	$20 \leq \rho_{ins,\beta} < 30$ dB	$\rho_{ins,\beta} \geq 30$ dB

instantaneous SNR value of the group ($\rho_{ins,\beta}$) with the predefined threshold values. For example, assume that there are two threshold values γ_1 and γ_2 where $\gamma_1 > \gamma_2$. If the average instantaneous received SNR of the group β ($\rho_{ins,\beta}$) is greater than threshold γ_1, *i.e.*, $\rho_{ins,\beta} > \gamma_1$, 16-QAM is used for modulation. In other case, if $\rho_{ins,\beta} < \gamma_2$, BPSK modulation is used for the group β. For $\gamma_2 < \rho_{ins,\beta} < \gamma_1$, QPSK modulation is chosen. Once the modulation type is determined, two different constellations for the selected modulation are applied to the subgroup according to IM bits. The modulation types and threshold values can be chosen in different ways. In this paper, we assume that we have six threshold set values, *i.e.*, $[\gamma_1, \gamma_2]$. Our different threshold set values, which are chosen empirically, used for modulation order selection are shown in Table 4.

3.2. SE of the proposed scheme

In the proposed scheme, SE value η is a random variable (RV) due to the random channel response. Its minimum and maximum values for $n = 4$, $k = 2$, $N = 128$, and $N_{CP} = 16$ are given as $\eta_{min} = (2 + 4) \times 32/(128 + 16) = 1.33$ bit/s/Hz and $\eta_{max} = (2+16)\times 32/(128+16) = 4$ bit/s/Hz. The η_{max} can only be achieved if all subcarriers are modulated with 16-QAM. This can be achieved if the average instantaneous received SNR values of all groups are greater than γ_1.

To calculate the average SE, we obtain CDF of the instantaneous received SNR. Since the channel coefficients are Rayleigh distributed, the received SNR is a χ^2-distributed random variable. The PDF of $\rho_{ins,\beta}$, or ρ shortly, is then given as in [31-(2.1.128)] by

$$f_\rho(\rho) = \frac{\rho}{\sigma^2} e^{\frac{-\rho^2}{2\sigma^2}} \tag{9}$$

where σ is the variance of AWGN. Also, its CDF is given as in [31-(2.1.128)] by

$$F_\rho(\rho) = 1 - e^{\frac{-\rho^2}{2\sigma^2}}, \ \rho \geq 0. \tag{10}$$

Then, by using a threshold set values $[\gamma_1, \gamma_2]$, the probability of usage of each modulation set at a specific SNR can be found as:

$$y_i = Pr[\gamma_i \leq \rho_{ins} \leq \gamma_{i+1}] = F_\rho(\gamma_{i+1}) - F_\rho(\gamma_i). \tag{11}$$

The average SE can be calculated by using (11) :

$$\eta = g\left(\frac{p_1 + \sum_{i=1}^{L} m_i y_i}{N + N_{CP}}\right) \tag{12}$$

where p_1, g and L represent the index bits, the number of subblocks and the number of the different modulation types. m_i and y_i denote number of transmitted bits by the selected modulation type and the probability of usage of the selected modulation type, respectively.

3.3. Computational complexity analysis of the proposed scheme

In the proposed system model, since the channel is perfectly known at Rx side, the modulation of each subblock is also known. For this reason, Rx should estimate the indices bits and symbols by using ML decoding as in (5) similar to DM-OFDM-IM system. However, the computational complexity increases for the proposed scheme compared to DM-OFDM-IM because one OFDM symbol can include many modulation types. One more important fact is that the computational complexity of our proposed system is lower or equal to that of the DM-OFDM-IM system while using the highest modulation level. If the average received instantaneous SNR of β subblock ($\rho_{ins,\beta}$) is higher than γ_1, 16-QAM is selected for this subblock. Because ML detector searches 262 144 possible realizations for 16-QAM, the computation time becomes relatively high. A similar case can be occurred when the threshold set value is selected as low. Unlike the previous one, if the received instantaneous SNR of β subblock ($\rho_{ins,\beta}$) is lower than γ_2 ($\rho_{ins,\beta}$ can be low or γ_2 can be selected as low), BPSK modulation type is selected for this group and the ML detector tries to find the minimum decision metrics by searching only 64 possible subblock realizations for BPSK.

Table 5
The number of possible realization in ML Computing for three different schemes for $n = 4$, $k = 2$ and $p_1 = 2$.

	BPSK mod.	QPSK mod.	16-QAM mod.
OFDM-IM	16	64	4 096
DM-OFDM-IM	64	1024	262 144
The proposed scheme		$\frac{4\times(y_1 2^4+y_2 4^4+y_3 16^4)}{y_1+y_2+y_3}$	

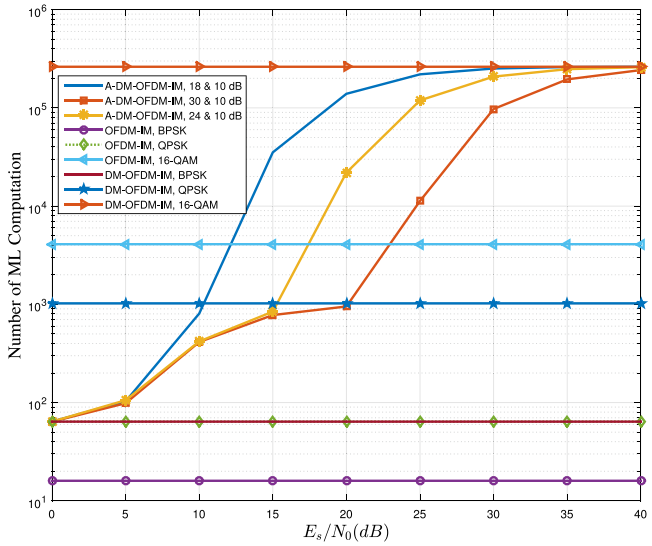

Fig. 6. Number of ML detector computation vs. E_s/N_0 for different threshold set values and different schemes.

As a conclusion, if the majority of the groups are modulated by BPSK modulation, the computation time will decrease, otherwise the computation time will increase as the usage percentage of 16-QAM increases. In other words, when the modulation order increases, the computation time will increase considerably.

Let $c = 2^{p_1}$ denotes the number of possible realizations of the selected active indices. While the computational complexity of the ML detector for OFDM-IM is $\sim \mathcal{O}(cM^k)$, the computational complexity of ML detector for DM-OFDM-IM is $\sim \mathcal{O}(cM^{2k})$ (or $\sim \mathcal{O}(cM^n)$).

Example. Assume that the parameters n and k are chosen as 4 and 2, respectively. For BPSK modulation, there are two possible symbols and four different positions for each symbol in each subblocks. Thus, 16 possible (symbol state) realizations should be checked in (5) to jointly estimate symbol and indices bits in OFDM-IM. The ML solution can be found by minimizing (5). In DM-OFDM-IM, for the same parameters, the number of possible subblock realizations ($2^4 \times 4 = 64$) is four times higher than that of OFDM-IM due to two different constellation alphabets (schemes). We calculate the computational complexity for OFDM-IM, DM-OFDM-IM and the proposed system for these parameters as shown in Table 5. In this table, y_i denotes the probability of usage of each modulation type (set). Moreover, in our simulations, ML detector should check $\frac{4\times(y_1 2^4+y_2 4^4+y_3 16^4)}{y_1+y_2+y_3}$ possible realizations.

Fig. 6 shows the number of computations of ML detector with respect to E_s/N_0 dB for different threshold set values and different schemes. As modulation order increases, the number of possible realizations, which ML detector has to calculate, also increases. As can be seen from Fig. 6, in DM-OFDM-IM with 16-QAM, ML detector requires the calculation of the highest number of possible realizations. Our proposed scheme converges this number when E_s/N_0 dB is greater than threshold set because of 16-QAM usage.

Table 6
Spectral efficiency for different schemes with different modulation type.

Cases	SE (bit/s/Hz)
OFDM-IM BPSK, $n = 4$, $k = 2$	0.89
OFDM-IM QPSK, $n = 4$, $k = 2$	1.33
OFDM-IM 16-QAM, $n = 4$, $k = 2$	2.22
DM-OFDM-IM BPSK, $n = 4$, $k = 2$	1.33
DM-OFDM-IM QPSK, $n = 4$, $k = 2$	2.22
DM-OFDM-IM 16-QAM, $n = 4$, $k = 2$	4
A-DM-OFDM-IM, $n = 4$, $k = 2$	$1.33 \leq \eta \leq 4$

Moreover, when the lowest threshold set, *i.e.* [18, 10] dB is selected, the number of possible realizations of ML detector increases earlier compared to other threshold set values. This is because switching point to 16-QAM from QPSK is very low. According to these curves, the computational load of ML detector of A-DM-OFDM-IM is always lower than that of DM-OFDM-IM with 16-QAM. Moreover, ML detector in OFDM-IM requires the minimum calculation count of possible realizations due to usage of single type constellation.

4. Simulation results

In the simulations, we assumed that our proposed system has a limited feedback channel from Rx to Tx in order to determine the suitable modulation type to enhance BER and SE. By using this limited feedback channel, Rx only sends the average CIR knowledge of each group instead of all CIR knowledge to Tx. In the simulations, we assume that OFDM signal is transmitted over a frequency-selective Rayleigh fading channel. The number of channel taps (ν) is selected as 10. Thus, CP length and IFFT length are chosen as $N_{CP} = 16$ and $N = 128$. For the sake of simplicity, we assumed $n = 4$ and $k = 2$ for all schemes.

We used different type of modulation schemes, such as BPSK, QPSK and 16-QAM, but the system can be extended by adding high order modulation types. Moreover, we have two different constellations for each type of modulation which are given in Fig. 5. In one OFDM symbol, all modulation types can be used according to instantaneous received SNR values of subcarriers groups. Switching between modulations is the result of comparing the average SNR value of the subcarrier group to a set of predefined threshold values.

Threshold selection is the most important factor on the trade-off between BER performance and the SE. In this paper, we choose six different threshold set values to select the modulation order. Table 6 shows the SE for OFDM-IM, DM-OFDM-IM and our proposed scheme for different modulation types.

Fig. 7 shows the BER performance of the proposed scheme with different threshold set values. As seen from Fig. 7, all curves have almost the same slope until $E_s/N_0 = 15$ dB. However, after this value the best performance can be obtained by using [30, 20] dB threshold set.

As we know that when the modulation order gets higher, the SE also increases, however the BER performance gets worse for the same SNR value. When the average instantaneous received SNR for subblock β ($\rho_{ins,\beta}$) is higher than 10 dB and 18 dB ([18, 10] dB), modulation type can be selected as QPSK and 16-QAM, respectively. We note that these selections are the lowest threshold values to increase the modulation order. As a consequence, the SE reaches the highest value while the BER performance becomes the worst.

Fig. 8 shows the theoretical and simulation results of the average SE variation versus E_s/N_0 for different threshold set values. As seen from Fig. 8, simulation results perfectly match the theoretical ones, which are calculated by (12), especially at low E_s/N_0 values.

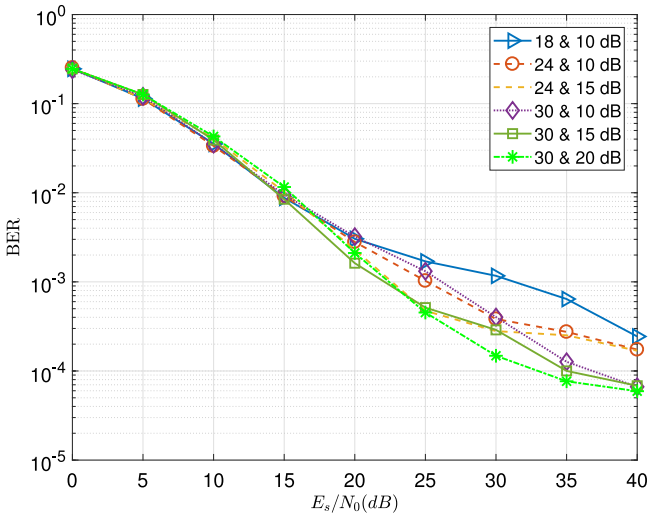

Fig. 7. BER performance vs. E_s/N_0 for different threshold set values.

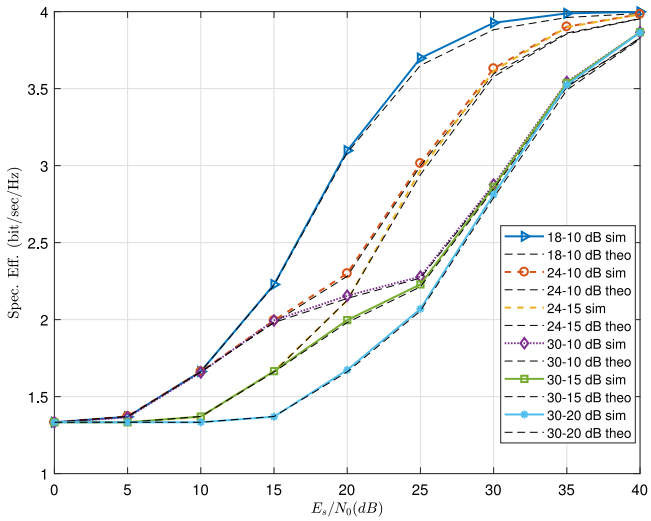

Fig. 8. Spectral efficiency vs. E_s/N_0 for different threshold values in dB.

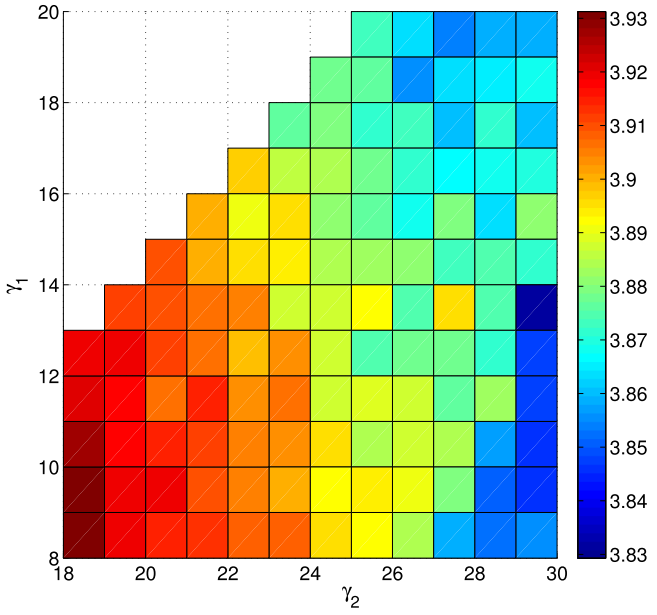

Fig. 9. SE variation with respect to $[\gamma_1, \gamma_2]$ in dB for $E_s/N_0 = 25$ dB.

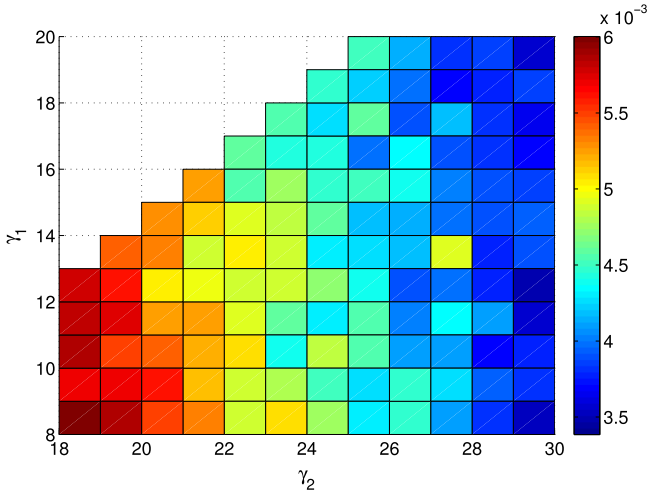

Fig. 10. BER variation with respect to $[\gamma_1, \gamma_2]$ in dB for $E_s/N_0 = 25$ dB.

Similarly, when the average instantaneous received SNR is higher than 20 dB and 30 dB ([30, 20]) dB, the modulation type can be selected as QPSK and 16-QAM, respectively. Compared to the previous situation, as a result of increasing the required instantaneous received SNR for transition from BPSK to QPSK, the SE decreases and the BER performance enhances. As its known, the error probability increases as the modulation level increases. For this reason, the BER performance becomes worse than the others if the threshold set value is chosen low. The best performance is obtained by using [30, 20] dB threshold set.

Figs. 9 and 10 illustrate the average SE and the average BER variations with respect to different threshold sets $[\gamma_1, \gamma_2]$ in a three dimensional plot. This threshold set consists of 156 elements and we assume that $E_s/N_0 = 25$ dB, γ_1 value increments from 18 to 30 dB and γ_2 value increments from 8 to 20 dB. Moreover, the trade-off between the SE and the average BER values can be seen from Figs. 9 and 10. High SE values can be obtained by using low threshold combinations. Moreover, the improvement of the average BER performance can be observed while moving threshold combinations towards higher values.

To make a fair comparison among all systems, all constellation alphabets (*Cons A* and *Cons B*) for each modulation are normalized to have unit average energy. In Fig. 11, we compare the BER performance of the proposed scheme with DM-OFDM-IM by using 16-QAM, QPSK and BPSK schemes. In computer simulations, we show that the proposed adaptive scheme always outperforms the classical DM-OFDM-IM with 16-QAM. However compared to DM-OFDM-IM with BPSK and QPSK, it still provides a better BER performance at particular SNR values. For example, in Fig. 11 the BER performance of A-DM-OFDM-IM with [30, 20] dB is better than DM-OFDM-IM with BPSK for SNR values between 5–32 dB.

It may seem questionable at first that the BER performance of the adaptive system is better than DM-OFDM-IM with BPSK. The reason for this is that in DM-OFDM-IM, BPSK modulation is used in each subblock regardless of whether the channel is high gain or not. However, the proposed scheme selects a modulation type among three possible modulation types, according to channel conditions due to its adaptive structure. Thus, more bits can be conveyed in the

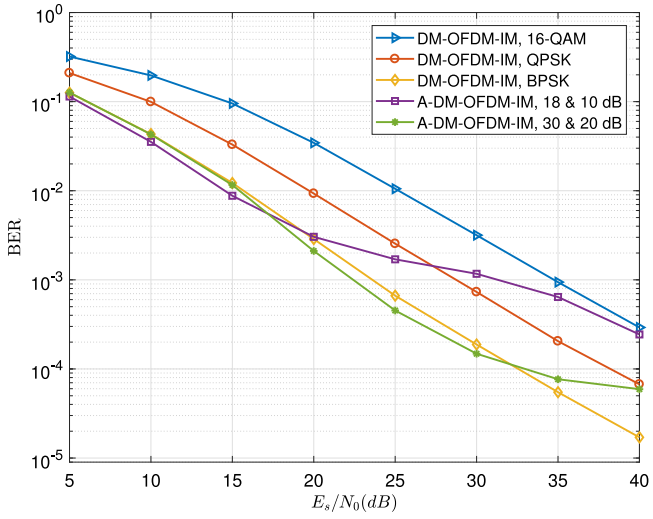

Fig. 11. The average BER vs. E_s/N_0 (dB) for different modulation schemes.

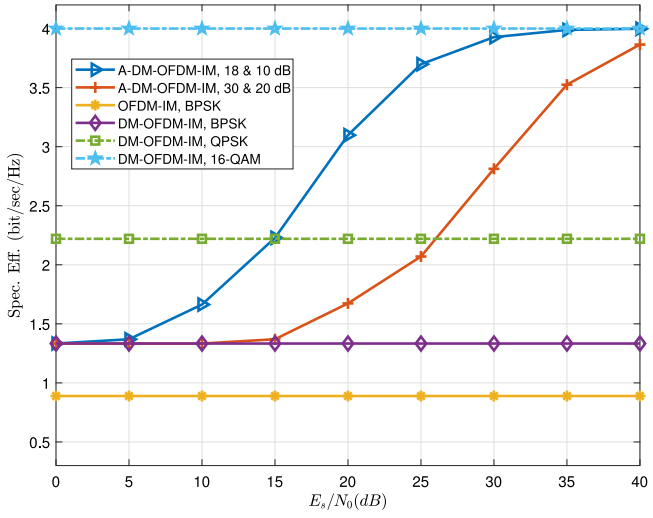

Fig. 12. The spectral efficiency vs. E_s/N_0 (dB) for different modulation schemes.

proposed scheme with subblocks that have a high received SNR, compared that of DM-OFDM-IM with BPSK.

Fig. 12 shows the SE variation with E_s/N_0 for different modulation schemes. As can be seen from Fig. 12, OFDM-IM with BPSK gives the minimum SE compared the other systems. Moreover, the proposed scheme with different threshold set values provide a better SE value compared to DM-OFDM-IM with BPSK ($n = 4$, $k = 2$). The SE values of the A-DM-OFDM-IM scheme with [18, 10] dB is better than that of the A-DM-OFDM-IM scheme with [30, 20] dB. However, both of them give higher SE values compared to DM-OFDM-IM with QPSK modulation when E_s/N_0 is greater than 26 dB. The highest SE value is obtained by DM-OFDM-IM with 16-QAM. Since there is a trade-off between SE and BER performance, we conclude that simulation results in Figs. 7 and 12 are consistent.

The performance of the proposed systems heavily depends on the CSI feedback. Until this point, we have assumed that the CSI is perfectly feedback from Rx to Tx. However, in practical situations, the assumption of the perfect CSI feedback may be unrealistic. The impact of imperfect feedback in an adaptive OFDM system is analyzed in [31]. The authors of this study assumed that the feedback knowledge of each subcarrier is conveyed with one bit

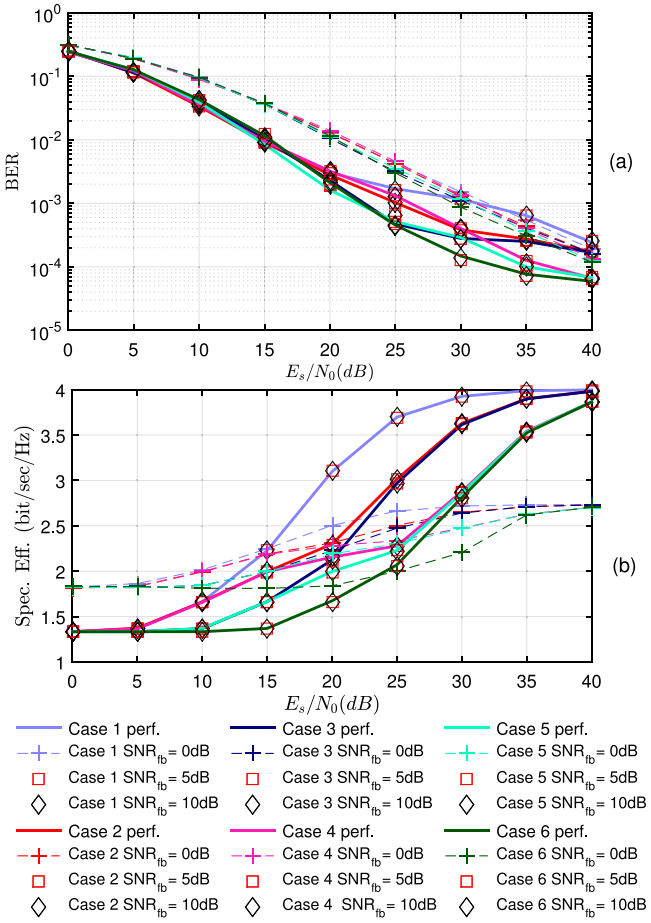

Fig. 13. Imperfect feedback channel effect on (a) BER and (b) SE vs. E_s/N_0 (dB) for all different threshold sets.

(*i.e.*, 0 or 1). In our system, Rx sends only the information of the selected modulation type of each subblock with 2 bits (due to having 3 modulation options), consequently, it conveys half of the feedback knowledge compared with that of [31].

In Fig. 13, we illustrated the impact of the imperfect feedback on the BER and SE performance of the proposed system for all threshold sets. Threshold set values are indicated as Case which is defined in Table 4. While solid-lines for each color represent the perfect feedback channel case, dot-lines for each color represent the case which SNR of feedback channel (SNR_{fb}) equal 0 dB. Square and diamond markers show $SNR_{fb} = 5$ dB and $SNR_{fb} = 10$ dB, respectively. As seen from Fig. 13, when SNR_{fb} increases, BER and SE results of imperfect channel close to the BER and SE results of the perfect case.

To extend our analysis on the BER performance of the proposed system for all SNR_{fb} values, we calculated MSE values by using BER results in the perfect feedback case and the imperfect case with different SNR values. The MSE result is given in Fig. 14 for two different threshold sets which gives the best and the worst BER results, *i.e.*, [30, 20] dB and [18, 10] dB, respectively. In this analysis, we assume that the feedback knowledge is transmitted with BPSK modulation over the noisy feedback channel with different SNR_{fb} values. In computer simulation, SNR of the channel from Tx to Rx is assumed to be constant (for each MSE step). As seen from Fig. 14, when the SNR value increases, MSE value decreases. We conclude from Fig. 14, that when the SNR is above 10 dB, the effect of the imperfect feedback on the BER performance of the proposed scheme is almost negligible.

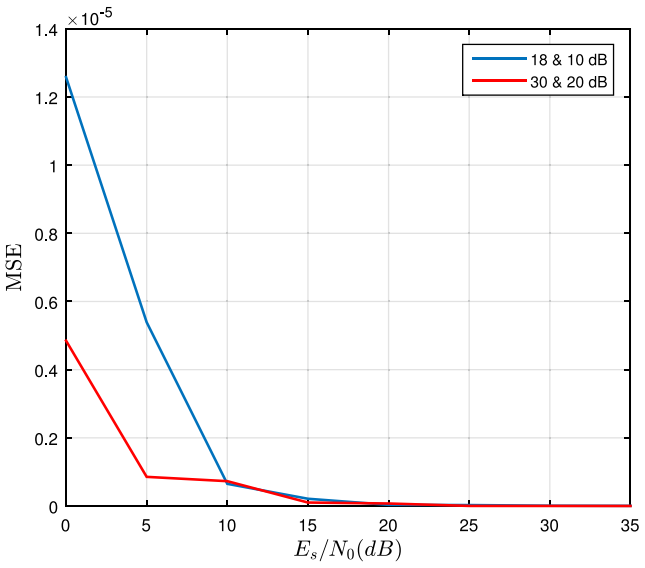

Fig. 14. MSE vs. E_s/N_0 (dB) for two different threshold sets.

5. Conclusion

In this paper, we have proposed a new adaptive modulation scheme for DM-OFDM-IM to enhance the average BER performance and SE according the channel condition. The proposed scheme divides the overall subcarrier into subgroups, and then each subgroup can be modulated by a different modulation scheme according the channel transfer function. We have demonstrated that the SE of the proposed system is superior compared to that of its OFDM-IM and DM-OFDM-IM counterparts under frequency selective Rayleigh channel. The SE of the A-DM-OFDM-IM scheme has been obtained by both theoretical calculations and computer simulations, which are in perfect agreement. The main advantage of the A-DM-OFDM-IM scheme is the selection of the appropriate threshold set, which may provide a higher SE or a lower BER.

Acknowledgments

This work has been supported by the Scientific and Technological Research Council of Turkey-TUBITAK, Grant Number: TUBITAK-BIDEB-2219 International Post-Doctoral Research Fellowship Program.

References

[1] A.A. Zaidi, R. Baldemair, H. Tullberg, H. Bjorkegren, L. Sundstrom, J. Medbo, C. Kilinc, I. Da Silva, Waveform and numerology to support 5G services and requirements, IEEE Commun. Mag. 54 (11) (2016) 90–98.
[2] A.A. Zaidi, R. Baldemair, In the race to 5G, CP-OFDM triumphs! available: https://www.ericsson.com/research-blog/in-race-to-5g-cp-ofdm-triumphs/ 54 (11), 2017, 90–98.
[3] R.Y. Mesleh, H. Haas, S. Sinanovic, C.W. Ahn, S. Yun, Spatial modulation, IEEE Trans. Veh. Technol. 57 (4) (2008) 2228–2241.
[4] E. Basar, Ü. Aygölü, E. Panayırcı, H.V. Poor, Orthogonal frequency division multiplexing with index modulation, IEEE Trans. Signal Process. 61 (22) (2013) 5536–5549.
[5] E. Basar, E. Panayırcı, Optical OFDM with index modulation for visible light communications, in: 2015 4th International Workshop on Optical Wireless Communications, (IWOW), IEEE, 2015, pp. 11–15.
[6] T. Mao, R. Jiang, R. Bai, Optical dual-mode index modulation aided OFDM for visible light communications, Opt. Commun. 391 (2017) 37–41.
[7] E. Basar, Multiple-input multiple-output OFDM with index modulation, IEEE Signal Process. Lett. 22 (12) (2015) 2259–2263.
[8] E. Basar, On multiple-input multiple-output OFDM with index modulation for next generation wireless networks, IEEE Trans. Signal Process. 64 (15) (2016) 3868–3878.
[9] B. Zheng, M. Wen, E. Basar, F. Chen, Multiple-input multiple-output OFDM with index modulation: Low-complexity detector design, IEEE Trans. Signal Process. 65 (11) (2017) 2758–2772.
[10] L. Wang, Z. Chen, Z. Gong, M. Wu, Space-frequency coded index modulation with linear-complexity maximum likelihood receiver in the MIMO-OFDM system, IEEE Signal Process. Lett. 23 (10) (2016) 1439–1443.
[11] R. Fan, Y.J. Yu, Y.L. Guan, Orthogonal frequency division multiplexing with generalized index modulation, in: Global Communications Conference, (GLOBECOM), IEEE, 2014, pp. 3880–3885.
[12] Y. Xiao, S. Wang, L. Dan, X. Lei, P. Yang, W. Xiang, OFDM with interleaved subcarrier-index modulation, IEEE Commun. Lett. 18 (8) (2014) 1447–1450.
[13] E. Basar, OFDM with index modulation using coordinate interleaving, IEEE Wirel. Commun. Lett. 4 (4) (2015) 381–384.
[14] M. Wen, B. Ye, E. Basar, Q. Li, F. Ji, Enhanced orthogonal frequency division multiplexing with index modulation, IEEE Trans. Wireless Commun. 16 (7) (2017) 4786–4801.
[15] E. Öztürk, E. Basar, H.A. Çirpan, Generalized frequency division multiplexing with flexible index modulation, IEEE Access 99 (2017) 1–1.
[16] E. Basar, M. Wen, R. Mesleh, M. Di Renzo, Y. Xiao, H. Haas, Index modulation techniques for next-generation wireless networks, IEEE Access 5 (2017) 16693–16746.
[17] T. Mao, Z. Wang, Q. Wang, S. Chen, L. Hanzo, Dual-mode index modulation aided OFDM, IEEE Access 5 (2017) 50–60.
[18] T. Mao, Q. Wang, Z. Wang, Generalized dual-mode index modulation aided OFDM, IEEE Commun. Lett. 21 (4) (2017) 761–764.
[19] M. Wen, E. Basar, Q. Li, B. Zheng, M. Zhang, Multiple-mode orthogonal frequency division multiplexing with index modulation, IEEE Trans. Commun. 65 (9) (2017) 3892–3906.
[20] Y. George, O. Amrani, Bit loading algorithms for OFDM, in: International Symposium on Information Theory, 2004. ISIT 2004. Proceedings, IEEE, 2004, 391–391.
[21] S. Ye, R.S. Blum, L.J. Cimini, Adaptive OFDM systems with imperfect channel state information, IEEE Trans. Wireless Commun. 5 (11) (2006) 3255–3265.
[22] A. Czylwik, Adaptive OFDM for wideband radio channels, in: Global Telecommunications Conference, 1996. GLOBECOM'96.'Communications: The Key to Global Prosperity, Vol. 1, IEEE, 1996, pp. 713–718.
[23] L. Piazzo, Fast algorithm for power and bit allocation in OFDM systems, Electron. Lett. 35 (25) (1999) 2173–2174.
[24] Z. Zhou, B. Vucetic, M. Dohler, Y. Li, MIMO systems with adaptive modulation, IEEE Trans. Veh. Technol. 54 (5) (2005) 1828–1842.
[25] A.N. Barreto, S. Furrer, Adaptive bit loading for wireless OFDM systems, in: 2001 12th IEEE International Symposium on Personal, Indoor and Mobile Radio Communications, Vol. 2, IEEE, 2001, pp. 88–92.
[26] J. Jang, K.B. Lee, Y.-H. Lee, Transmit power and bit allocations for OFDM systems in a fading channel, in: Global Telecommunications Conference, 2003. GLOBECOM'03. IEEE, Vol. 2, IEEE, 2003, pp. 858–862.
[27] M.-S. Alouini, A.J. Goldsmith, Adaptive modulation over nakagami fading channels, Wirel. Pers. Commun. 13 (1–2) (2000) 119–143.
[28] T. Keller, L. Hanzo, Adaptive orthogonal frequency division multiplexing schemes, ACST Summit, Rhodos, Greece, 1998, pp. 794–799.
[29] Z. Bouida, A. Ghrayeb, K.A. Qaraqe, Adaptive spatial modulation for spectrally-efficient MIMO systems, in: Wireless Communications and Networking Conference, (WCNC), IEEE, 2014, pp. 583–587.
[30] P. Yang, Y. Xiao, L. Li, Q. Tang, Y. Yu, S. Li, Link adaptation for spatial modulation with limited feedback, IEEE Trans. Veh. Technol. 61 (8) (2012) 3808–3813.
[31] Y. Rong, S.A. Vorobyov, A.B. Gershman, The impact of imperfect one bit per subcarrier channel state information feedback on adaptive OFDM wireless communication systems, in: IEEE 60th Vehicular Technology Conference, 2004. VTC2004-Fall. 2004, Vol. 1, 2004, pp. 626–630. http://dx.doi.org/10.1109/VETECF.2004.1400083.

Sultan Aldırmaz Çolak received the B.S degree in Electronics and Communications Engineering from Kocaeli University, Kocaeli 2004 and the M.S. and PhD degrees in Yildiz Technical University (YTU), Istanbul 2006 and 2012, respectively. She was a visiting research scholar in the Department of Electrical and Computer Engineering of University of South Florida for the spring and summer of 2009. She is currently an Assistant Professor in the Electronics and Communications Engineering Department of Kocaeli University, Kocaeli, Turkey. Her research interests are in time–frequency signal processing, and communications theory.

Yusuf Acar received the B.S.E. degree (with honors), M.S.E. degree and Ph.D. degrees in Electrical and Electronics Engineering from Istanbul University, Istanbul, Turkey, in 2008, 2011 and 2015, respectively. From 2009 to 2015 he was employed as a research and teaching assistant at the faculty of the Department of Electrical and Electronics Engineering, Istanbul Kültür University. In 2015, he joined the same faculty as an Assistant Professor. He was a visiting scholar at the Indiana University- Purdue University Fort Wayne (IPFW), USA, between the June 2012 and September 2012. He is also a researcher now at the IPFW, Fort Wayne, USA, between the September 2017 and September 2018. His general research interests cover communication theory, estimation theory, statistical signal processing, and information theory. His current research activities are focused on wireless communication concepts with specific attention to equalization and channel estimation for spread-spectrum and multicarrier systems. His current research activities are focused on software-defined platforms.

Ertugrul Basar received his B.S. degree with high honors from Istanbul University, Turkey, in 2007, and his M.S. and Ph.D. degrees from Istanbul Technical University in 2009 and 2013, respectively. He spent the academic year 2011–2012 at the Department of Electrical Engineering, Princeton University, New Jersey. Currently, he is an associate professor at Istanbul Technical University, Electronics and Communication Engineering Department, and a member of the Wireless Communication Research Group. He was the recipient of the Istanbul Technical University Best Ph.D. Thesis Award in 2014 and has won three Best Paper Awards. He is an Associate Editor for IEEE Communications Letters and IEEE Access, an editor for Physical Communication, a regular reviewer for various IEEE journals, and has served as a TPC member for several conferences. His primary research interests include MIMO systems, index modulation, cooperative communications, OFDM, and visible light communications.